Finer features for functional microdevices

Micromachines can be created with higher resolution using two-photon absorption.

Compared with light or electron-beam lithography, the virtue of two-photon photopolymerization[1] as a tool for making microdevices lies in its three-dimensional capability, which has found application in photonic devices[2–4] and micromachines[1,5,6] with feature sizes close to the diffraction limit. Here we show that the diffraction limit can be exceeded by nonlinear effects to give a subdiffraction-limit spatial resolution of 120 nanometres. This allows functional micromachines to be created and shifts the working wavelength of photonic and opto-electronic devices into the visible and near-infrared region.

Commercially available resin (SCR500; JSR, Japan), consisting of urethane acrylate monomers and oligomers as well as photoinitiators, is transparent to an infrared laser and allows it to penetrate deeply. The resin can be photopolymerized by using two-photon absorption (TPA)[7–9] to create three-dimensional structures. By pinpoint-scanning the laser focus according to preprogrammed patterns, designs can be faithfully replicated to matter structures.

Figure 1a–f shows scanning electron micrographs of 'micro-bull' sculptures. These 10-μm-long, 7-μm-high bulls are the smallest model animals ever made artificially, and are about the size of a red blood cell. The tiny volume attainable for such micromachines would allow them to be transported to locations inside the human body through even the smallest blood vessels, for example to deliver clinical treatments.

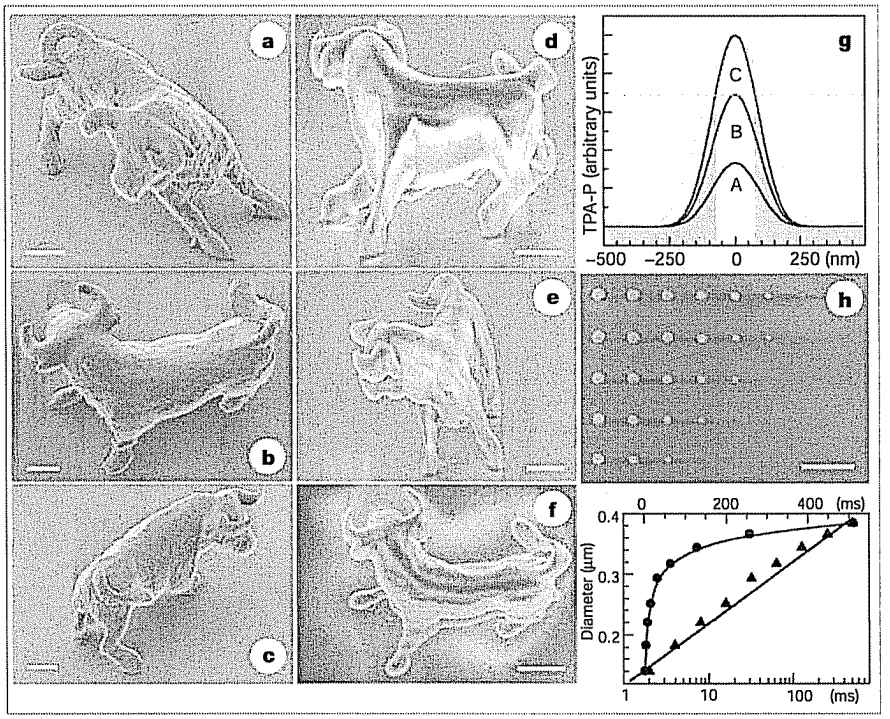

Figure 1 Microfabrication and nanofabrication at subdiffraction-limit resolution. A titanium sapphire laser operating in mode-lock at 76 MHz and 780 nm with a 150-femtosecond pulse width was used as an exposure source. The laser was focused by an objective lens of high numerical aperture (~1.4). **a–c,** Bull sculpture produced by raster scanning; the process took 180 min. **d–f,** The surface of the bull was defined by two-photon absorption (TPA; that is, surface-profile scanning) and was then solidified internally by illumination under a mercury lamp, reducing the TPA-scanning time to 13 min. **g,** Achievement of subdiffraction-limit resolution, where A, B and C respectively denote the laser-pulse energy below, at and above the TPA-polymerization threshold (dashed line). The yellow line represents the range of single-photon absorption. TPA-P, TPA probability. **h,** Scanning electron micrograph of voxels formed at different exposure times and laser-pulse energies. **i,** Dependence of lateral spatial resolution on exposure time. The laser-pulse energy was 137 pJ. The same data are presented using both logarithmic (triangles; bottom axis) and linear (circles; top axis) coordinates, to show the logarithmic dependence and threshold behaviour of TPA photopolymerization. Scale bars, 2 μm.

To depict the tiny features of our microbulls, a fabrication accuracy of about 150 nm was needed, which we achieved by using nonlinear processes of the photochemical reactions involved. Polymerization occurred only in the vicinity of the focal spot and the size of solidified voxels (three-dimensional volume elements) was reduced because of the quadratic dependence of TPA probability on the photon fluence density. Furthermore, photogenerated radicals in this volume were subject to scavenging by dissolved oxygen molecules[10], so polymerization reactions were not initiated and propagated if the exposure energy was less than a critical value.

This property defined a TPA threshold and excluded the low-intensity lobe (the zero-order edge and the subsidiary maxima of the Airy pattern) from polymerization and thus further reduced the voxel size (Fig. 1g). The diffraction limit imposed by Rayleigh criteria was simply a measure of focal-spot size, and did not put any restraint on the actual size of solidified voxels. We were thus able to design voxels of any small size by choosing an appropriate laser-pulse energy and exposure time, because only the region with energy above the TPA threshold was solidified (Fig. 1h).

A logarithmic dependence of voxel size on exposure time (Fig. 1i) results from the exponential decay of the oligomer/monomer

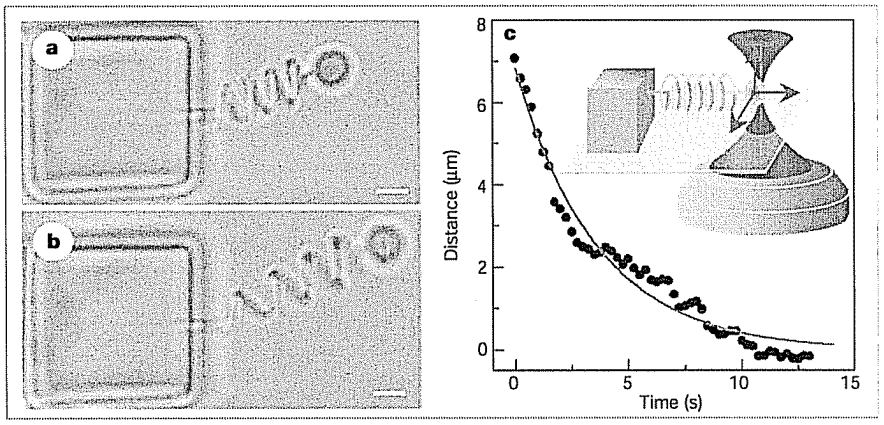

Figure 2 Functional micro-oscillator system, in which not only the spring but also the cubic anchor and the bead were produced using our two-photon absorption system. The oscillator was kept in ethanol so that the buoyancy would balance gravity and eliminate bead–substrate friction. **a, b,** The spring in its original (**a**) and extended (**b**) states. Scale bars, 2 μm. **c,** Restoring curve of the damping oscillation; inset, diagram showing driving of the oscillator by using laser trapping.

concentration during exposure. Our spatial resolution of 120 nm is superior to that achieved by conventional rapid-laser prototyping and by conventional TPA fabrication[1–8] (smaller voxels can be formed, but it is difficult for isolated voxels to appear in the same scanning electron micrograph; in an actual fabrication, the spatial resolution may be better than 120 nm).

As an example of subdiffraction-limit fabrication, we produced a micro-oscillator, which must be the smallest functional micromechanical system produced (note that the microspring shown in Fig. 2a, b has a spiral diameter of only 300 nm). To operate such a minute spring, we converted it into an oscillator by fixing one end to an anchor attached to a glass substrate and polymerizing a bead (diameter, 3 μm) at the other end. We used laser-trapping force[11,12] to capture the bead, pulled the spring (Fig. 2b), and then released it from its displacement (Fig. 2c, inset) to set the vibration in motion (see movie in supplementary information).

An 820-nm, 19-mW laser offered a trapping force of about 3 piconewtons, which is equivalent to a $20g$ acceleration of the bead, where g is the acceleration due to gravity. However, because of the large specific surface of the oscillator, viscosity heavily damped the oscillation. We assume that the damping force is proportional to the velocity of the bead movement, $f_{vis} = 6\pi\eta r v$ (Stokes' law), where η (1.084×10^{-3} pascals per second at 25 °C) is the liquid viscosity and v is the bead velocity. The spring damping oscillation can be expressed as $m\mathrm{d}^2x/\mathrm{d}t^2 = -kx - 6\pi\eta r(\mathrm{d}x/\mathrm{d}t)$, where m (1.6×10^{-14} kg) is the bead mass and k is the spring constant to be determined. Figure 2c shows the bead displacement during spring restoration against time, from which the spring constant was deduced to be 8.2 nN m^{-1}. Such soft springs are directly applicable to the investigation of the mechanical properties of micro-objects.

Satoshi Kawata, Hong-Bo Sun, Tomokazu Tanaka, Kenji Takada
Department of Applied Physics, Osaka University, Suita, Osaka 565-0871, Japan
e-mail: kawata@ap.eng.osaka-u.ac.jp

1. Maruo, S., Nakamura, O. & Kawata, S. *Opt. Lett.* **22**, 132–134 (1997).
2. Sun, H.-B., Matsuo, S. & Misawa, H. *Appl. Phys. Lett.* **74**, 786–788 (1999).
3. Cumpston, B. H. *et al. Nature* **398**, 51–54 (1999).
4. Sun, H.-B. *et al. Appl. Phys. Lett.* **79**, 1–3 (2001).
5. Maruo, S. & Kawata, S. *IEEE J. Microelectromech. Syst.* **7**, 411–415 (1998).
6. Sun, H.-B. *et al. Opt. Lett.* **25**, 1110–1112 (2000).
7. Parthenopoulos, D. A. & Rentzepis, P. M. *Science* **245**, 843–845 (1989).
8. Denk, W., Strickler, J. H. & Webb, W. W. *Science* **248**, 73–76 (1990).
9. Wu, E. S., Strickler, J. H., Harrell, W. R. & Webb W. W. *Proc. SPIE* **1674**, 776–782 (1992).
10. Flory, P. J. *Principals of Polymer Chemistry* (Cornell Univ. Press, New York, 1952).
11. Ashkin, A. *Phys. Rev. Lett.* **24**, 156–159 (1970).
12. Inouye, Y., Shoji, S., Furukawa, H., Nakamura, O. & Kawata, S. *Jpn J. Appl. Phys.* **37**, L684–L686 (1998).

Supplementary information is available on *Nature*'s website (http://www.nature.com).

Sex determination

Viviparous lizard selects sex of embryos

No one suspected that temperature-dependent sex determination (TSD)[1–3], whereby the sex of embryos depends on the temperature at which they develop, might occur in viviparous (live-bearing) reptiles, because thermoregulation in the mother results in relatively stable, raised gestation temperatures. But here we show that developing embryos of the actively thermoregulating viviparous skink *Eulamprus tympanum* are subject to TSD, offering the mother the chance to select the sex of her offspring and a mechanism to help to balance sex ratios in wild populations.

Sex determination is the programmed cascade of events through which an undifferentiated gonad develops into a testis or an ovary. In vertebrates, sex is determined either by a genotypic mechanism at the time of fertilization, which depends only on genetic factors, or by environmental factors that act after fertilization. Species that are subject to TSD provide an example of the latter mechanism and usually lack heteromorphic sex chromosomes. Reptiles rely on either temperature or genetic factors to influence the sex of their offspring[4].

E. tympanum is a medium-sized scincid lizard found in high-elevation habitats in southeastern Australia, with a litter size of one to five young[5]. As no species within *Eulamprus* has detectable heteromorphic sex chromosomes, we investigated whether *E. tympanum* might be subject to TSD. We maintained mothers at different laboratory temperatures and used palpation of the hemipenes[6] and histology of neonatal gonads[7,8] to establish sex. To our surprise, we discovered that gestation temperature has a highly significant effect on sex ($P < 0.001$), with warmer temperatures giving rise to male offspring (Fig. 1).

Active thermoregulation by pregnant viviparous lizards distinguishes the thermal environment of development from that in oviparous species. A combination of active thermoregulation and TSD provides the female lizard with the opportunity to select the sex of her offspring. In the laboratory, all females provided with unlimited conditions for thermoregulation maintained body temperatures of 32 °C and produced exclusively male offspring. Equal sex ratios resulted from natural gestation in two field seasons.

We do not understand the mechanism by which females select body temperature to give equal sex ratios in the field; the implication is that thermoregulatory conditions may be restricted. Alternatively, other factors, such as unbalanced adult sex ratios, may result in mothers selectively thermoregulating to produce offspring that help to balance the population sex ratio. A viviparous skink from Tasmania adjusts the sex ratio of its offspring according to the operational sex ratio of the adult population[9]; presumably, TSD provides the mechanism for selection of neonatal gender by the mothers. Our population of *E. tympanum* has an adult sex ratio that is not significantly different from unity[10] in the field, where they produce an equal sex ratio of neonates; however, our laboratory population was all female and produced all sons when given the opportunity to thermoregulate.

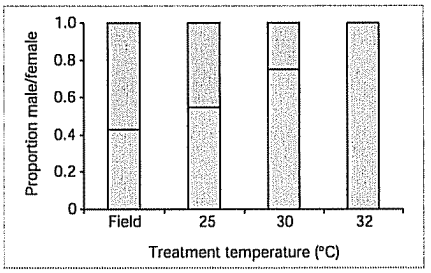

Figure 1 Influence of gestation temperature on the sex ratio of offspring of the viviparous lizard *Eulamprus tympanum*. Females maintained at 32 °C ($n = 21$) for the duration of pregnancy gave birth to exclusively male offspring ($n = 55$); those maintained at 30 °C ($n = 20$) gave birth to predominantly male offspring ($n = 58$; 75% were male); those maintained at 25 °C ($n = 11$) gave birth to offspring of both sexes ($n = 20$; 55% were male); those undergoing most of their gestation in the field ($n = 24$) also produced a mix of sexes ($n = 58$; 43% were male). Orange portions of bars represent male offspring; blue portions represent female offspring.

TSD may explain the fact that *E. tympanum*, like many other viviparous taxa, is restricted to alpine regions. The warmer temperatures further down the slopes would encourage production of exclusively male offspring and lead to the eventual extinction of those populations. A combination of alpine distribution and TSD is likely to be a problem in the event of rapid climate change or global warming, as these species may not be able to evolve rapidly enough to compensate[11]. For alpine species, there can be no retreat to cooler climates, so a rise in environmental temperature would result in increased production of males. Models predict a temperature rise of 4 °C by 2100 (ref. 12), which could seriously alter the sex ratio and lead to extinction of species such as *E. tympanum*.

Kylie A. Robert, Michael B. Thompson
School of Biological Sciences and Institute of Wildlife Research, University of Sydney, New South Wales 2006, Australia
e-mail: krobert@bio.usyd.edu.au

1. Bull, J. J. *Q. Rev. Biol.* **55**, 3–21 (1980).